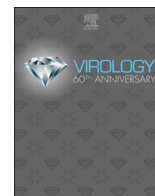




Since January 2020 Elsevier has created a COVID-19 resource centre with free information in English and Mandarin on the novel coronavirus COVID-19. The COVID-19 resource centre is hosted on Elsevier Connect, the company's public news and information website.

Elsevier hereby grants permission to make all its COVID-19-related research that is available on the COVID-19 resource centre - including this research content - immediately available in PubMed Central and other publicly funded repositories, such as the WHO COVID database with rights for unrestricted research re-use and analyses in any form or by any means with acknowledgement of the original source. These permissions are granted for free by Elsevier for as long as the COVID-19 resource centre remains active.



## The FDA-approved gold drug auranofin inhibits novel coronavirus (SARS-COV-2) replication and attenuates inflammation in human cells

Hussin A. Rothan<sup>\*\*</sup>, Shannon Stone, Janhavi Natekar, Pratima Kumari, Komal Arora, Mukesh Kumar<sup>\*</sup>

Department of Biology, College of Arts and Sciences, Georgia State University, Atlanta, 30303, Georgia



### ARTICLE INFO

#### Keywords:

SARS-COV-2  
COVID-19  
Auranofin  
Antiviral  
Anti-inflammatory

### ABSTRACT

SARS-COV-2 has recently emerged as a new public health threat. Herein, we report that the FDA-approved drug, auranofin, inhibits SARS-COV-2 replication in human cells at low micro molar concentration. Treatment of cells with auranofin resulted in a 95% reduction in the viral RNA at 48 h after infection. Auranofin treatment dramatically reduced the expression of SARS-COV-2-induced cytokines in human cells. These data indicate that auranofin could be a useful drug to limit SARS-CoV-2 infection and associated lung injury due to its antiviral, anti-inflammatory and anti-reactive oxygen species (ROS) properties. Further animal studies are warranted to evaluate the safety and efficacy of auranofin for the management of SARS-COV-2 associated disease.

Gold-based compounds have shown promising activity against a wide range of clinical conditions and microorganism infections. Auranofin, a gold-containing triethyl phosphine, is an FDA-approved drug for the treatment of rheumatoid arthritis since 1985 (Roder and Thomson, 2015). It has been investigated for potential therapeutic application in a number of other diseases including cancer, neurodegenerative disorders, HIV/AIDS, parasitic infections and bacterial infections (Roder and Thomson, 2015; Harbut et al., 2015). Auranofin was approved by FDA for phase II clinical trials for cancer therapy (Hou et al., 2018; Oh et al., 2017; Rigobello et al., 2009). Oral auranofin was effective in rodent models of various parasitic infections (Leitsch, 2017; Capparelli et al., 2017). A preclinical study showed that auranofin significantly reduces HIV load in combination with antiretroviral therapy (Lewis et al., 2011). A clinical trial is ongoing to develop auranofin as a drug candidate to reduce the latent viral reservoir in patients with HIV infection utilizing the role of auranofin in redox-sensitive cell death pathways (Diaz et al., 2019; Chirullo et al., 2013).

The mechanism of action of auranofin involves the inhibition of redox enzymes such as thioredoxin reductase, induction of endoplasmic reticulum (ER) stress and subsequent activation of the unfolded protein response (UPR) (Harbut et al., 2015; May et al., 2018; Wiederhold et al., 2017; Thangamani et al., 2016). Inhibition of these redox enzymes leads to cellular oxidative stress and intrinsic apoptosis (Lugea et al., 2017; Hetz, 2012). In addition, auranofin is an anti-inflammatory drug that reduces cytokines production and stimulate cell-mediated

immunity (Walz et al., 1983). It has been reported that auranofin interferes with the Interleukin 6 (IL-6) signaling by inhibiting phosphorylation of JAK1 and STAT3 (Han et al., 2008; Kim et al., 2007). The dual inhibition of inflammatory pathways and thiol redox enzymes by auranofin makes it an attractive candidate for cancer therapy and treating microbial infections.

Coronaviruses are a family of enveloped viruses with positive sense, single-stranded RNA genomes (Rothan and Byrareddy, 2020). SARS-CoV-2, the causative agent of COVID-19, is closely related to severe acute respiratory syndrome coronavirus (SARS-CoV-1) (Rothan and Byrareddy, 2020; Mehta et al., 2020). It is known that ER stress and UPR activation contribute significantly to the viral replication and pathogenesis during a coronavirus infection (Fung and Liu, 2014). Infection with SARS-COV-1 increases the expression of the ER protein folding chaperons GRP78, GRP94 and other ER stress related genes to maintain protein folding (Tang et al., 2005). Cells overexpressing the SARS-COV spike protein and other viral proteins exhibit high levels of UPR activation (Siu et al., 2014; Sung et al., 2009). Thus, inhibition of redox enzymes such as thioredoxin reductase and induction of ER stress by auranofin could significantly affect SARS-COV-2 protein synthesis (Rothan and Kumar, 2019).

In addition, SARS-COV-2 infection causes acute inflammation and neutrophilia that leads to a cytokine storm with over expression of IL-6, TNF-alpha, monocyte chemoattractant protein (MCP-1) and reactive oxygen species (ROS) (Mehta et al., 2020). The severe COVID-19 illness

<sup>\*</sup> Corresponding author. Department of Biology, College of Arts and Sciences, Georgia State University, 145 Piedmont Ave SE, Atlanta, GA, 30303, Georgia.

<sup>\*\*</sup> Corresponding author. Department of Biology, College of Arts and Sciences, Georgia State University, 145 Piedmont Ave SE, Atlanta, GA, 30303, Georgia.

E-mail addresses: [hrothan@gsu.edu](mailto:hrothan@gsu.edu) (H.A. Rothan), [mkumar8@gsu.edu](mailto:mkumar8@gsu.edu) (M. Kumar).

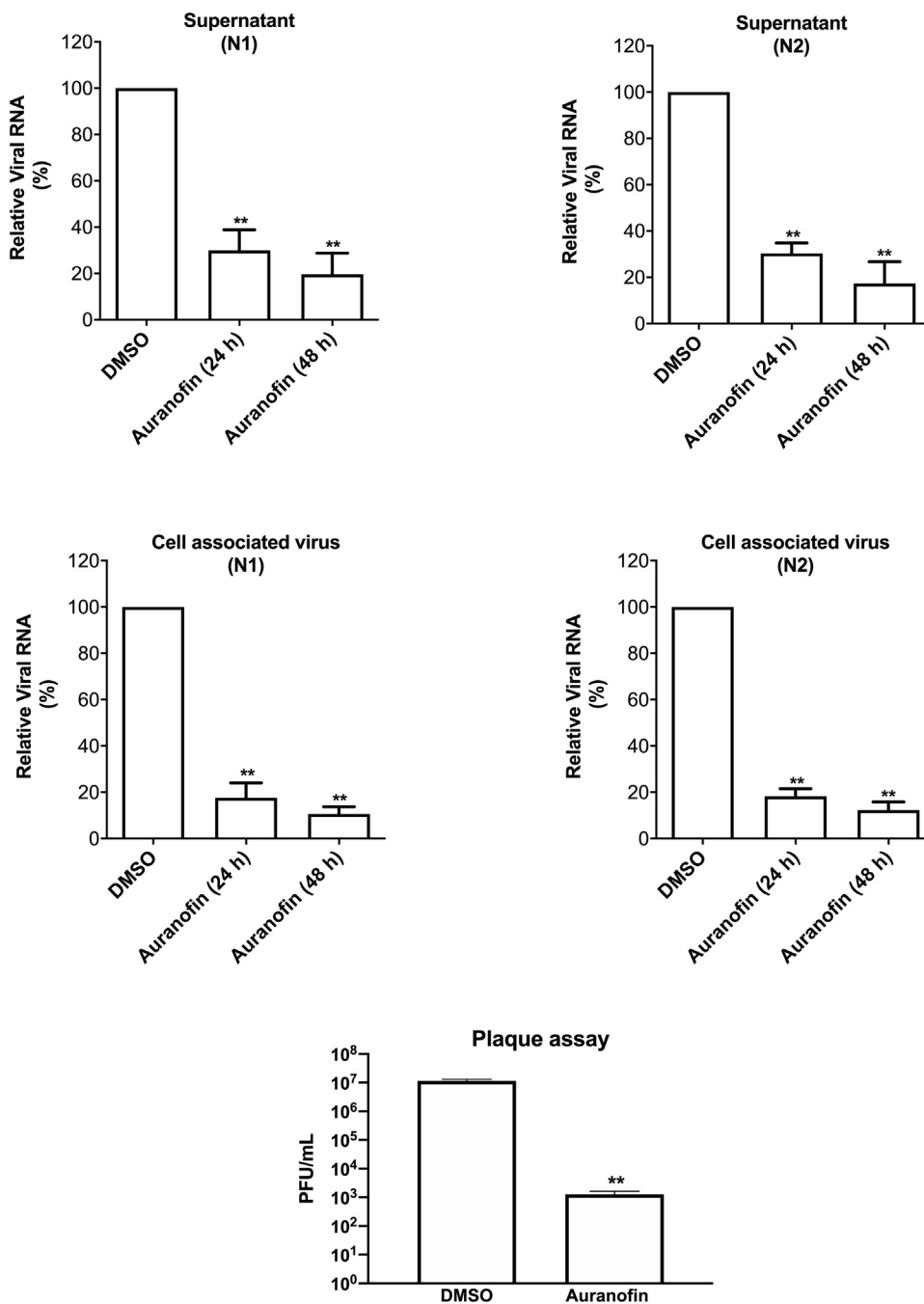


**Fig. 1. Auranofin inhibits replication of SARS-CoV-2 in human cells.** Huh7 cells were infected with SARS-CoV-2 at a multiplicity of infection (MOI) of 1 for 2 h and treated with 4  $\mu$ M of auranofin or with 0.1% DMSO. Cell pellets and culture supernatants were collected at 24 and 48 h after infection and viral RNA levels were measured by RT-PCR using primers and probe targeting the SARS-CoV-2 N1 region and the SARS-CoV-2 N2 region. The cellular RNA extracted from infected cells was quantified, normalized and viral RNA levels per  $\mu$ g of total cellular RNA were calculated. The results were identical for both set of primers showing dramatic reduction in viral RNA at both 24 and 48 h. SARS-CoV-2 infectivity titers were measured in cell culture supernatants at 48 h after infection by plaque assay. Data represent the mean  $\pm$  SEM, representing two independent experiments conducted in duplicate, *t*-test  $p < 0.001$ .

represents a devastating inflammatory lung disorder due to cytokines storm that is associated with multiple organ dysfunction leading to high mortality (Mehta et al., 2020; Sarzi-Puttini et al., 2020). Taken together, these studies suggest that auranofin could mitigate SARS-CoV-2 infection and associated lung damage due to its anti-viral, anti-inflammatory and anti-ROS properties.

We investigated the anti-viral activity of auranofin against SARS-CoV-2 and its effect on virus-induced inflammation in human cells. We infected Huh7 cells with SARS-CoV-2 (USA-WA1/2020) at a multiplicity of infection (MOI) of 1 for 2 h, followed by the addition of 4  $\mu$ M of auranofin. DMSO (0.1%) was used as control (the solvent was used to prepare drug stock). We used Huh7 cells in this study as these cells are highly permissive for SARS-CoV-2 replication. Cell culture supernatants and cell lysates were collected at 24 and 48 h after infection. Virus RNA copies were measured by RT-PCR using two separate primers specific for the viral N1 region and N2 region (Rothan et al., 2019;

Kumar et al., 2017). As depicted in Fig. 1, treatment of cells with auranofin resulted in a 70% reduction in the viral RNA in the supernatants compared to the DMSO at 24 h after infection. At 48 h, there was an 85% reduction in the viral RNA in the supernatants compared to the DMSO. Similarly, the levels of intracellular viral RNA decreased by 85% at 24 h and 95% at 48 h in auranofin-treated cells compared to the DMSO-treated cells. Both set of primers showed nearly identical results. We next assayed virus titers in cell culture supernatants by plaque assay. Treatment with auranofin significantly reduced SARS-CoV-2 infectivity titers in cell culture supernatants at 48 h after infection (Fig. 1).

To determine the effective concentration of auranofin that inhibits 50% of viral replication ( $EC_{50}$ ), we treated SARS-CoV-2 infected Huh7 cells with serial dilutions of auranofin. Supernatants and cell lysates were collected at 48 h after infection and viral RNA was quantified by RT-PCR. The data were plotted in graphs using non-linear regression

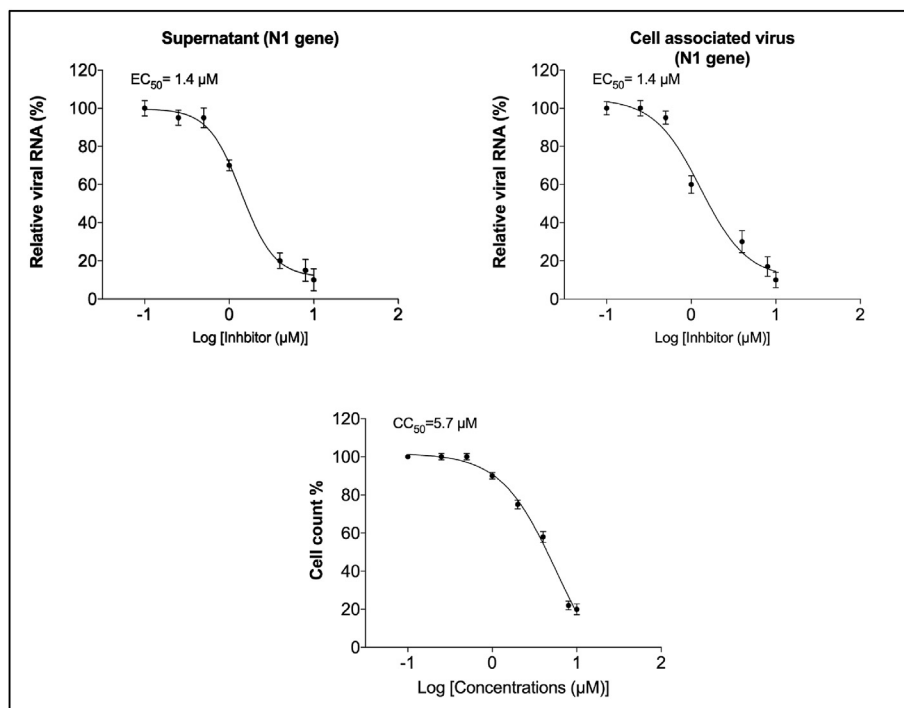


**Fig. 2.** Dose-dependent reduction in SARS-CoV-2 RNA in the auranofin-treated cells: The SARS-CoV-2 infected Huh7 cells were treated with serial dilutions of auranofin (0.1–10  $\mu\text{M}$ ). Viral RNA in the cell pellets and culture supernatants were quantified by RT-PCR using primers and probe targeting the SARS-CoV-2 N1. The data were plotted in graphs using non-linear regression model (GraphPad software). Auranofin inhibited virus replication in the infected cells at  $\text{EC}_{50}$  of approximately 1.4  $\mu\text{M}$ . The cytotoxic concentration of 50% was approximately 5.7  $\mu\text{M}$ . Data represent two independent experiments conducted in duplicate.

model (GraphPad software). At 48 h, there was a dose-dependent reduction in viral RNA levels in the auranofin-treated cells. Fig. 2 represents the  $\text{EC}_{50}$  values of auranofin treatment against SARS-CoV-2 infected Huh7 cells. Auranofin inhibited virus replication in the infected cells at  $\text{EC}_{50}$  of approximately 1.4  $\mu\text{M}$ . It is important to note that in this study, we used 20 to 100-times more virus dose (MOI of 1) to infect the cells compared to the recently published reports on anti-viral activities of chloroquine, hydroxychloroquine and remdesivir against SARS-CoV-2 in vitro (Wang et al., 2020; Liu et al., 2020).

To assess the effect of auranofin on inflammatory response during SARS-CoV-2 infection, we measured the levels of key cytokines in auranofin and DMSO-treated cells at 24 and 48 h after infection (Natekar et al., 2019). SARS-CoV-2 infection induces a strong up-regulation of IL-6, IL-1 $\beta$ , TNF $\alpha$  and NF- $\kappa\text{B}$  in Huh7 cells (Fig. 3). Treatment with auranofin dramatically reduced the expression of SARS-CoV-2-induced cytokines in Huh7 cells. SARS-CoV-2 infection resulted in a 200-fold increase in the mRNA expression of IL-6 at 48 h after infection compared to corresponding mock-infected cells. In contrast, there was only a 2-fold increase in expression of IL-6 in auranofin-treated cells. TNF- $\alpha$  levels increased by 90-fold in the DMSO-treated cells at 48 h after infection, but this increase was absent in the auranofin-treated cells. Similarly, no increase in the expression of IL-1 $\beta$  and NF- $\kappa\text{B}$  was observed in the auranofin-treated cells.

**Taken together** these results demonstrate that auranofin inhibits replication of SARS-CoV-2 in human cells at low micro molar concentration. We also demonstrate that auranofin treatment resulted in significant reduction in the expression of cytokines induced by virus infection. These data indicate that auranofin could be a useful drug to limit SARS-CoV-2 infection and associated lung injury. Further animal studies are warranted to evaluate the safety and efficacy of auranofin for the management of SARS-CoV-2 associated disease.

## 1. Methods

### 1.1. SARS-CoV-2 infection and drug treatment

In this study, we used a novel SARS-CoV-2 (USA-WA1/2020) isolated from an oropharyngeal swab from a patient in Washington, USA

(BEI NR-52281). Virus strain was amplified once in Vero E6 cells and had titers of  $5 \times 10^6$  plaque-forming units (PFU)/mL. Huh7 cells (human liver cell line) were grown in DMEM (Gibco) supplemented with 5% heat-inactivated fetal bovine serum. Cells were infected with SARS-CoV-2 or PBS (Mock) at a multiplicity of infection (MOI) of 1 for 2 h (Natekar et al., 2019; Azouz et al., 2019; Kim et al., 2018; Krause et al., 2019). Cells were washed twice with PBS and media containing different concentrations of auranofin (0.1–10  $\mu\text{M}$ , Sigma) or DMSO (0.1%, Sigma) was added to cells. Supernatants and cell lysates were harvested at 24 and 48 h after infection. The cytotoxicity of auranofin in Huh7 cells was measured using trypan blue method as described previously (Varghese and Busselberg, 2014). Briefly, Huh7 cells were treated with different concentrations of auranofin (0.1–10  $\mu\text{M}$ ) for 48 h and percentage cell numbers were quantified using trypan blue.

### 1.2. Virus quantification

Virus infectivity titers were measured in cell culture supernatants by plaque formation assay using Vero cells as we described previously (Natekar et al., 2019). Virus RNA levels were analyzed in the supernatant and cell lysates by quantitative reverse transcription-polymerase chain reaction (qRT-PCR). RNA from cell culture supernatants was extracted using a Viral RNA Mini Kit (Qiagen) and RNA from cell lysates was extracted using a RNeasy Mini Kit (Qiagen) as described previously (Natekar et al., 2019). The cellular RNA extracted from infected cells was quantified, normalized and viral RNA levels per  $\mu\text{g}$  of total cellular RNA were calculated. qRT-PCR was used to measure viral RNA levels using previously published primers and probes specific for the SARS-CoV-2. Forward (5'-GACCCCAAAATC AGCGAAAT-3'), reverse (5'-TCTGGTTACTGCCAGTTGAATCTG-3'), probe, (5'-FAM-ACCCGCATTACGTTTGGTGGACC-BHQ1-3') targeting the SARS-CoV-2 N1 region and Forward (5'-TTACAAACATTGGCCGCAAA-3'), reverse (5'-GCGCGACATTCGGAAGAA3'), probe, (5'-FAM-ACAATTTGCCCCA GCGCTTCAG-BHQ1-3') targeting the SARS-CoV-2 N2 region (Integrated DNA Technologies). Viral RNA copies were determined after comparison with a standard curve produced using serial 10-fold dilutions of SARS-CoV-2 RNA (Kumar et al., 2017; Kim et al., 2018).

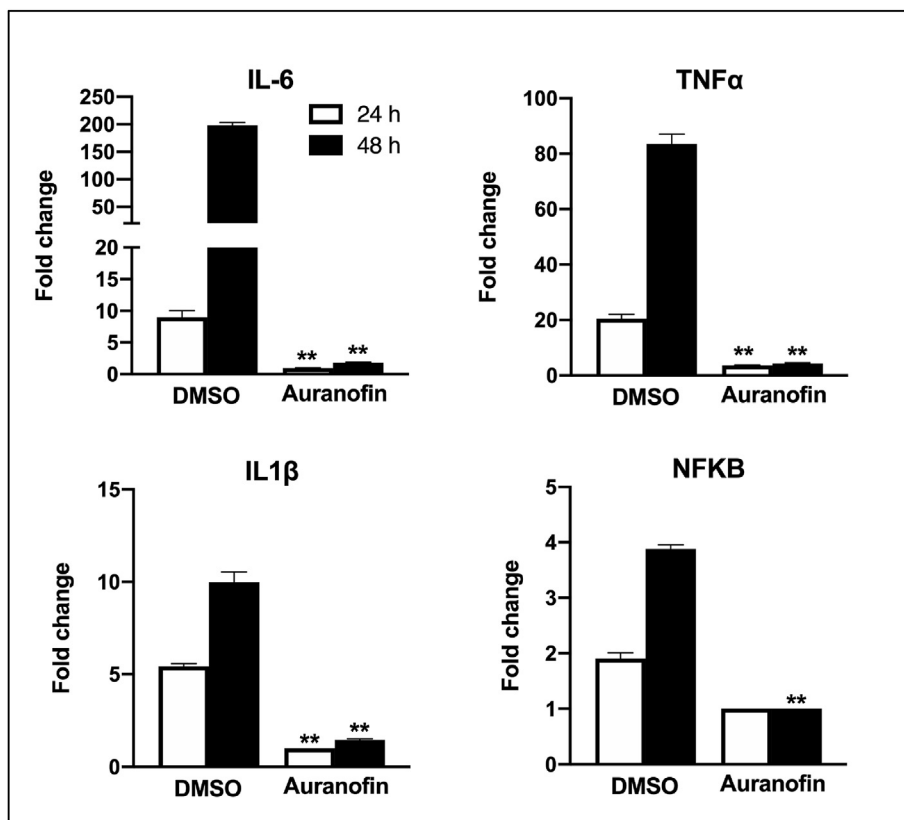


**Fig. 3. Auranofin treatment dramatically reduced the expression of SARS-COV-2-induced cytokines in human cells:** mRNA levels of IL-6, IL-1 $\beta$ , TNF $\alpha$  and NF-kB were determined using qRT-PCR at 24 and 48 h after infection. The fold change in infected cells compared to corresponding controls was calculated after normalizing to the GAPDH gene. Data represent the mean  $\pm$  SEM, representing two independent experiments conducted in duplicate.

**Table 1**  
Primer sequences used for qRT-PCR.

Gene (Accession No.)	Primer Sequence (5'-3')
<b>IL-1<math>\beta</math> (NM_000576)</b>	
Forward	AGCACCTTCTTTCCCTTCATC
Reverse	GGACCAGACATCACCAAGC
<b>IL-6 (NM_000600)</b>	
Forward	CCAGGAGCCCAGCTATGAAC
Reverse	CCCAGGGAGAAGGCAACTG
<b>NFKB (NM_003998)</b>	
Forward	TCCTTCTTTGACTCATACA
Reverse	TGCCCTCACATACATAAAG
<b>TNF (NM_000594)</b>	
Forward	CCTGCCCAATCCCTTTATT
Reverse	CCCTAAGCCCCCAATTCTCT

### 1.3. Cytokine analysis

For mRNA analysis of IL-6, IL-1 $\beta$ , TNF $\alpha$  and NF-kB, cDNA was prepared from RNA isolated from the cell lysates using a iScript<sup>TM</sup> cDNA Synthesis Kit (Bio-Rad, Hercules, CA, USA), and qRT-PCR was conducted as described previously (Natekar et al., 2019). The fold change in infected cells compared to corresponding controls was calculated after normalizing to the GAPDH gene. The primer sequences used for qRT-PCR are listed in Table 1.

### CRedit authorship contribution statement

**Hussin A. Rothan:** Conceptualization, Methodology, Validation, Formal analysis, Writing - original draft. **Shannon Stone:** Methodology, Validation, Formal analysis. **Janhavi Natekar:** Methodology, Validation, Formal analysis. **Pratima Kumari:** Methodology, Validation, Formal analysis. **Komal Arora:** Formal analysis, Writing - original draft. **Mukesh Kumar:** Investigation,

Conceptualization, Formal analysis, Writing - original draft, Writing - review & editing, Resources, Supervision, Funding acquisition.

### Declaration of competing interest

Authors declare no conflict of Interest.

### Acknowledgements

This work was supported by a grant (R21NS099838) from National Institute of Neurological Disorders and Stroke, grant (R21OD024896) from the Office of the Director, National Institutes of Health, and Institutional funds.

### References

- Azouz, F., Arora, K., Krause, K., Nerurkar, V.R., Kumar, M., 2019. Integrated MicroRNA and mRNA profiling in zika virus-infected neurons. *Viruses* 11 (2). <https://doi.org/10.3390/v11020162>. PubMed PMID: 30781519; PMCID: 6410042.
- Capparelli, E.V., Bricker-Ford, R., Rogers, M.J., McKerrow, J.H., Reed, S.L., 2017. Phase I clinical trial results of auranofin, a novel antiparasitic agent. *Antimicrob. Agents Chemother.* 61 (1). <https://doi.org/10.1128/AAC.01947-16>. PubMed PMID: 27821451; PMCID: 5192119.
- Chirullo, B., Sgarbanti, R., Limongi, D., Shytaj, I.L., Alvarez, D., Das, B., Boe, A., DaFonseca, S., Chomont, N., Liotta, L., Petricoin, E.L., Norelli, S., Pelosi, E., Garaci, E., Savarino, A., Palamara, A.T., 2013. A candidate anti-HIV reservoir compound, auranofin, exerts a selective 'anti-memory' effect by exploiting the baseline oxidative status of lymphocytes. *Cell Death Dis.* 4, e944. <https://doi.org/10.1038/cddis.2013.473>. PubMed PMID: 24309931; PMCID: 3877546.
- Diaz, R.S., Shytaj, I.L., Giron, L.B., Obermaier, B., Della Libera Jr., E., Galinskas, J., Dias, D., Hunter, J., Janini, M., Gosuen, G., Ferreira, P.A., Sucupira, M.C., Maricato, J., Fackler, O., Lusic, M., Savarino, A., Group, S.W., 2019. Potential impact of the antirheumatic agent auranofin on proviral HIV-1 DNA in individuals under intensified antiretroviral therapy: results from a randomised clinical trial. *Int. J. Antimicrob. Agents* 54 (5), 592–600. <https://doi.org/10.1016/j.ijantimicag.2019.08.001>. PubMed PMID: 31394172.
- Fung, T.S., Liu, D.X., 2014. Coronavirus infection, ER stress, apoptosis and innate immunity. *Epub* 2014/07/06. *Front. Microbiol.* 5, 296. <https://doi.org/10.3389/fmicb.2014.00296>. PubMed PMID: 24987391; PMCID: PMC4060729.
- Han, S., Kim, K., Kim, H., Kwon, J., Lee, Y.H., Lee, C.K., Song, Y., Lee, S.J., Ha, N., Kim, K.,



2008. Auranofin inhibits overproduction of pro-inflammatory cytokines, cyclooxygenase expression and PGE2 production in macrophages. *Arch Pharm. Res. (Seoul)* 31 (1), 67–74. <https://doi.org/10.1007/s12272-008-1122-9>. PubMed PMID: 18277610.
- Harbut, M.B., Vilcheze, C., Luo, X., Hensler, M.E., Guo, H., Yang, B., Chatterjee, A.K., Nizet, V., Jacobs Jr., W.R., Schultz, P.G., Wang, F., 2015. Auranofin exerts broad-spectrum bactericidal activities by targeting thiol-redox homeostasis. *Epub 2015/04/02. Proc. Natl. Acad. Sci. U. S. A.* 112 (14), 4453–4458. <https://doi.org/10.1073/pnas.1504022112>. PubMed PMID: 25831516; PMCID: PMC4394260.
- Hetz, C., 2012. The unfolded protein response: controlling cell fate decisions under ER stress and beyond. *Nat. Rev. Mol. Cell Biol.* 13 (2), 89–102. <https://doi.org/10.1038/nrm3270>. PubMed PMID: 22251901.
- Hou, G.X., Liu, P.P., Zhang, S., Yang, M., Liao, J., Yang, J., Hu, Y., Jiang, W.Q., Wen, S., Huang, P., 2018. Elimination of stem-like cancer cell side-population by auranofin through modulation of ROS and glycolysis. *Cell Death Dis.* 9 (2), 89. <https://doi.org/10.1038/s41419-017-0159-4>. PubMed PMID: 29367724; PMCID: 5833411.
- Kim, N.H., Lee, M.Y., Park, S.J., Choi, J.S., Oh, M.K., Kim, I.S., 2007. Auranofin blocks interleukin-6 signalling by inhibiting phosphorylation of JAK1 and STAT3. *Immunology* 122 (4), 607–614. <https://doi.org/10.1111/j.1365-2567.2007.02679.x>. PubMed PMID: 17645497; PMCID: 2266044.
- Kim, J.A., Seong, R.K., Kumar, M., Shin, O.S., 2018. Favipiravir and ribavirin inhibit replication of asian and african strains of zika virus in different cell models. *Epub 2018/02/10. Viruses* 10 (2). <https://doi.org/10.3390/v10020072>. PubMed PMID: 29425176; PMCID: PMC5850379.
- Krause, K., Azouz, F., Nakano, E., Nerurkar, V.R., Kumar, M., 2019. Deletion of pregnancy zone protein and murinoglobulin-1 restricts the pathogenesis of west Nile virus infection in mice. *Front. Microbiol.* 10, 259. <https://doi.org/10.3389/fmicb.2019.00259>. PubMed PMID: 30814992; PMCID: 6381297.
- Kumar, M., Krause, K.K., Azouz, F., Nakano, E., Nerurkar, V.R., 2017. A Guinea pig model of Zika virus infection. *Virol. J.* 14 (1), 75. <https://doi.org/10.1186/s12985-017-0750-4>. PubMed PMID: 28399888; PMCID: PMC5387205.
- Leitsch, D., 2017. Drug susceptibility testing in microaerophilic parasites: cysteine strongly affects the effectivities of metronidazole and auranofin, a novel and promising antimicrobial. *Int. J. Parasitol. Drugs and Drug Resist.* 7 (3), 321–327. <https://doi.org/10.1016/j.ijpddr.2017.09.001>. PubMed PMID: 28910741; PMCID: 5595233.
- Lewis, M.G., DaFonseca, S., Chomont, N., Palamara, A.T., Tardugno, M., Mai, A., Collins, M., Wagner, W.L., Yalley-Ogunro, J., Greenhouse, J., Chirullo, B., Norelli, S., Garaci, E., Savarino, A., 2011. Gold drug auranofin restricts the viral reservoir in the monkey AIDS model and induces containment of viral load following ART suspension. *AIDS* 25 (11), 1347–1356. <https://doi.org/10.1097/QAD.0b013e328347bd77>. PubMed PMID: 21505294.
- Liu, J., Cao, R., Xu, M., Wang, X., Zhang, H., Hu, H., Li, Y., Hu, Z., Zhong, W., Wang, M., 2020. Hydroxychloroquine, a less toxic derivative of chloroquine, is effective in inhibiting SARS-CoV-2 infection in vitro. *Cell discovery* 6, 16. <https://doi.org/10.1038/s41421-020-0156-0>. PubMed PMID: 32194981; PMCID: 7078228.
- Lugea, A., Gerloff, A., Su, H.Y., Xu, Z., Go, A., Hu, C., French, S.W., Wilson, J.S., Apte, M.V., Waldron, R.T., Pandolf, S.J., 2017. The combination of alcohol and cigarette smoke induces endoplasmic reticulum stress and cell death in pancreatic acinar cells. *Gastroenterology* 153 (6), 1674–1686. <https://doi.org/10.1053/j.gastro.2017.08.036>. PubMed PMID: 28847752; PMCID: 5705421.
- May, H.C., Yu, J.J., Guentzel, M.N., Chambers, J.P., Cap, A.P., Arulanandam, B.P., 2018. Repurposing auranofin, ebensen, and PX-12 as antimicrobial agents targeting the thioredoxin system. *Front. Microbiol.* 9, 336. <https://doi.org/10.3389/fmicb.2018.00336>. PubMed PMID: 29556223; PMCID: 5844926.
- Mehta, P., McAuley, D.F., Brown, M., Sanchez, E., Tattersall, R.S., Manson, J.J., Hlth Across Speciality Collaboration Uk, 2020. COVID-19: consider cytokine storm syndromes and immunosuppression. *Epub 2020/03/21. Lancet* 395 (10229), 1033–1034. [https://doi.org/10.1016/S0140-6736\(20\)30628-0](https://doi.org/10.1016/S0140-6736(20)30628-0). PubMed PMID: 32192578.
- Natekar, J.P., Rothan, H.A., Arora, K., Strate, P.G., Kumar, M., 2019. Cellular microRNA-155 regulates virus-induced inflammatory response and protects against lethal west Nile virus infection. *Epub 2019/12/22. Viruses* 12 (1). <https://doi.org/10.3390/v12010009>. PubMed PMID: 31861621.
- Oh, B.M., Lee, S.J., Cho, H.J., Park, Y.S., Kim, J.T., Yoon, S.R., Lee, S.C., Lim, J.S., Kim, B.Y., Choe, Y.K., Lee, H.G., 2017. Cystatin SN inhibits auranofin-induced cell death by autophagic induction and ROS regulation via glutathione reductase activity in colorectal cancer. *Cell Death Dis.* 8 (3), e2682. <https://doi.org/10.1038/cddis.2017.100>. PubMed PMID: 28300829; PMCID: 5386512.
- Rigobello, M.P., Gandin, V., Folda, A., Rundlof, A.K., Fernandes, A.P., Bindoli, A., Marzano, C., Bjornstedt, M., 2009. Treatment of human cancer cells with selenite or tellurite in combination with auranofin enhances cell death due to redox shift. *Free Radic. Biol. Med.* 47 (6), 710–721. <https://doi.org/10.1016/j.freeradbiomed.2009.05.027>. PubMed PMID: 19486940.
- Roder, C., Thomson, M.J., 2015. Auranofin: repurposing an old drug for a golden new age. *Drugs R* 15 (1), 13–20. <https://doi.org/10.1007/s40268-015-0083-y>. PubMed PMID: 25698589; PMCID: 4359176.
- Rothan, H.A., Byrareddy, S.N., 2020. The epidemiology and pathogenesis of coronavirus disease (COVID-19) outbreak. *Epub 2020/03/03. J. Autoimmun.* 102433. <https://doi.org/10.1016/j.jaut.2020.102433>. PubMed PMID: 32113704.
- Rothan, H.A., Kumar, M., 2019. Role of endoplasmic reticulum-associated proteins in flavivirus replication and assembly complexes. *Epub 2019/09/25. Pathogens* 8 (3). <https://doi.org/10.3390/pathogens8030148>. PubMed PMID: 31547236; PMCID: PMC6789530.
- Rothan, H.A., Arora, K., Natekar, J.P., Strate, P.G., Brinton, M.A., Kumar, M., 2019. Z-DNA-Binding protein 1 is critical for controlling virus replication and survival in west Nile virus encephalitis. *Epub 2019/10/02. Front. Microbiol.* 10, 2089. <https://doi.org/10.3389/fmicb.2019.02089>. PubMed PMID: 31572318; PMCID: PMC6749019.
- Sarzi-Puttini, P., Giorgi, V., Sirotti, S., Marotto, D., Ardizzone, S., Rizzardini, G., Antinori, S., Galli, M., 2020. COVID-19, cytokines and immunosuppression: what can we learn from severe acute respiratory syndrome? *Clin. Exp. Rheumatol.* 38 (2), 337–342. PubMed PMID: 32202240.
- Siu, K.L., Chan, C.P., Kok, K.H., Woo, P.C., Jin, D.Y., 2014. Comparative analysis of the activation of unfolded protein response by spike proteins of severe acute respiratory syndrome coronavirus and human coronavirus HKU1. *Cell Biosci.* 4 (1), 3. <https://doi.org/10.1186/2045-3701-4-3>. PubMed PMID: 24410900; PMCID: 3930072.
- Sung, S.C., Chao, C.Y., Jeng, K.S., Yang, J.Y., Lai, M.M., 2009. The 8ab protein of SARS-CoV is a luminal ER membrane-associated protein and induces the activation of ATF6. *Virology* 387 (2), 402–413. <https://doi.org/10.1016/j.virol.2009.02.021>. PubMed PMID: 19304306; PMCID: 7103415.
- Tang, B.S., Chan, K.H., Cheng, V.C., Woo, P.C., Lau, S.K., Lam, C.C., Chan, T.L., Wu, A.K., Hung, I.F., Leung, S.Y., Yuen, K.Y., 2005. Comparative host gene transcription by microarray analysis early after infection of the Huh7 cell line by severe acute respiratory syndrome coronavirus and human coronavirus 229E. *J. Virol.* 79 (10), 6180–6193. <https://doi.org/10.1128/JVI.79.10.6180-6193.2005>. PubMed PMID: 15858003; PMCID: 1091719.
- Thangamani, S., Mohammad, H., Abushahba, M.F., Sobreira, T.J., Seleem, M.N., 2016. Repurposing auranofin for the treatment of cutaneous staphylococcal infections. *Int. J. Antimicrob. Agents* 47 (3), 195–201. <https://doi.org/10.1016/j.ijantimicag.2015.12.016>. PubMed PMID: 26895605; PMCID: 4792765.
- Varghese, E., Busselberg, D., 2014. Auranofin, an anti-rheumatic gold compound, modulates apoptosis by elevating the intracellular calcium concentration ([Ca<sup>2+</sup>]<sub>i</sub>) in mcf-7 breast cancer cells. *Cancers* 6 (4), 2243–2258. <https://doi.org/10.3390/cancers6042243>. PubMed PMID: 25383481; PMCID: 4276964.
- Walz, D.T., DiMartino, M.J., Griswold, D.E., Intoccia, A.P., Flanagan, T.L., 1983. Biologic actions and pharmacokinetic studies of auranofin. *Am. J. Med.* 75 (6A), 90–108. [https://doi.org/10.1016/0002-9343\(83\)90481-3](https://doi.org/10.1016/0002-9343(83)90481-3). PubMed PMID: 6318557.
- Wang, M., Cao, R., Zhang, L., Yang, X., Liu, J., Xu, M., Shi, Z., Hu, Z., Zhong, W., Xiao, G., 2020. Remdesivir and chloroquine effectively inhibit the recently emerged novel coronavirus (2019-nCoV) in vitro. *Cell Res.* 30 (3), 269–271. <https://doi.org/10.1038/s41422-020-0282-0>. PubMed PMID: 32020029; PMCID: 7054408.
- Wiederhold, N.P., Patterson, T.F., Srinivasan, A., Chaturvedi, A.K., Fothergill, A.W., Wormley, F.L., Ramasubramanian, A.K., Lopez-Ribot, J.L., 2017. Repurposing auranofin as an antifungal: in vitro activity against a variety of medically important fungi. *Virulence* 8 (2), 138–142. <https://doi.org/10.1080/21505594.2016.1196301>. PubMed PMID: 27268469; PMCID: 5354159.